Limnol. Oceanogr., 50(5), 2005, 1612–1619

Shear-induced convective mixing in bottom boundary layers on slopes

Andreas Lorke[1]
Limnological Research Center, EAWAG, CH-6047 Kastanienbaum, Switzerland

Frank Peeters
Limnological Institute, University of Konstanz, D-78464 Konstanz, Germany

Alfred Wüest
Limnological Research Center, EAWAG, CH-6047 Kastanienbaum, Switzerland

Abstract

Field data from a stratified lake demonstrate that buoyancy-driven convective mixing can be an important mechanism for the formation of well-mixed bottom boundary layers (BBLs) on slopes. Convective turbulence is caused by differential transport of stratified water masses along the slope of a basin. Because the current velocity usually decreases toward the sediment, water at some distance from the bottom is transported faster than is water below. During upslope flow, this process leads to transport of heavier water on top of lighter water and hence to unstable stratification within the BBLs. Analogously, strong BBL stratification occurs during downslope flow. High-frequency acoustic Doppler current profiler (ADCP) and temperature measurements in the BBLs of a lake revealed the cyclic occurrence of convective turbulence driven by periodic across-slope currents of internal seiching. The estimated maximum buoyancy flux within the BBLs was in good agreement with the highest observed dissipation rates of turbulent kinetic energy. This suggests that, in our specific case, classical bottom shear production and the mentioned buoyancy-driven (convective) production contributed by similar amounts to the turbulent kinetic energy.

It is a frequently observed feature of many stratified water bodies that a well-mixed bottom boundary layer (BBL) exists directly above the sediment surface. The height of such well-mixed layers varies between a few meters in lakes and reservoirs (Gloor et al. 2000; Hondzo and Haider 2004; Lemckert et al. 2004) to several tens of meters in oceans (Caldwell 1978; Lentz and Trowbridge 1991). The turbulent kinetic energy (TKE) required to generate and maintain such mixed layers is usually assumed to be produced by the bottom friction of basin- or large-scale currents (Fricker and Nepf 2000; Wüest et al. 2000), shoaling and critical reflection of high-frequency internal waves (Thorpe 1997; Imberger 1998), or the interaction of large-scale currents with rough topography (Rudnick et al. 2003).

Enhanced mixing along the boundaries has been demonstrated in numerous studies (Macintyre et al. 1999; Ledwell et al. 2000; Garrett 2003). Moreover, tracer measurements in lakes (Goudsmit et al. 1997) and ocean basins (Ledwell and Bratkovich 1995; Ledwell and Hickey 1995) revealed the potential importance of boundary mixing for basin-scale transport processes (Imberger 1998; Müller and Garrett 2004).

The empirical fact that the lower part of the BBL is usually well mixed (Caldwell 1978) can be related to the no-flux boundary condition at the sediment surface. Phillips (1970) and Wunsch (1970) showed that isopycnals must intersect the sediment surface at a right angle to fulfill this boundary condition. Further, they showed that on slopes a steady (secondary) circulation can be generated, which results in a net upslope transport of heavier water (Thorpe 1987; Garrett 1991; Imberger and Ivey 1993). Experimental evidence of this buoyancy-driven transport is rare, because the associated current velocities are only a small addition to mean (e.g., tidal) currents. Observations on the continental shelf, however, have revealed asymmetries in the characteristics of the BBL between up- and downwelling flow (Weatherly and Martin 1978; Trowbridge and Lentz 1991).

A different mechanism, capable of generating buoyancy-driven convective mixing in BBLs on slopes, has been proposed by Lorke et al. (2002) and Wüest and Lorke (2003*a*). As schematically illustrated in Fig. 1, this mechanism is associated with upwelling on slopes in stratified basins. The decrease of the cross-slope current velocity toward the sediment surface (e.g., law-of-the-wall) leads to differential transport of water masses and results in a net flow of colder water on top of warmer water (Fig. 1). We term this process ''shear-induced convection'' throughout the rest of this article. Evidence for the occurrence of convectively driven mixing in BBLs was presented through numerical simulations by Slinn and Levine (2003), as well as in recent observations on the continental shelf by Moum et al. (2004). Various flows, such as baroclinic motions (internal seiches),

[1] To whom correpsondence should be addressed. Present address: Limnological Institute, University of Konstanz, Mainaustrasse 252, D-78464 Konstanz, Germany (andreas.lorke@uni-konstanz.de).

Acknowledgments

We thank M. Schurter and D. Finger for their great help in the field. The constructive input from two reviewers significantly improved the clarity of the manuscript; D. Richter, M. Schmid, and D. McGinnis provided helpful comments; and M. Stubbs kindly corrected the English.

The work was financially supported by the Swiss National Science Foundation (grants 2000-067091.01 and 200020-103827.1) and by EAWAG.

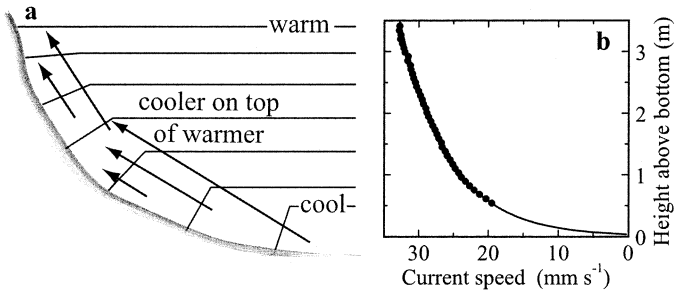

Fig. 1. (a) Schematic of the generation mechanism for shear-induced convective mixing by differential transport of water masses within the BBL on slopes of stratified basins. The decrease in current velocity toward the sediment surface (shown in b) results in the transport of denser (cooler) water upward and on top of lighter (warmer) water and hence in convectively driven mixing.

tides, Ekman transport, or wind-driven circulation can cause such slope-parallel flows.

The mechanism for the generation of shear-induced convection, as proposed above, is very similar to tidal straining in regions of freshwater influence (Simpson et al. 1990; Simpson 1997), in which the bottom is flat but the density gradients are horizontal. The cycling between stable and unstable stratification induced by the shearing motions of tidal currents in such systems was termed ''strain-induced periodic stratification'' (Simpson et al. 1990). It is associated with recurrent enhanced turbulence and mixing during the phase of unstable stratification when buoyancy acts as an additional source of TKE (Stacey et al. 1999; Rippeth et al. 2001).

In this article we present detailed observations of the periodic occurrence of convective mixing on the sloping bottom of a lake. Unstable stratification was produced by oscillating cross-slope currents driven by internal seiching.

Measurements and data analysis

Study site—Measurements were carried out in Lake Alpnach, a small (4.76 km^2) sub-basin of Lake Lucerne in Central Switzerland. Lake Alpnach has an elliptical shape with axis lengths of 5 and 1.5 km and a maximum depth of 34 m. The bottom shape along the main axis of the lake and the positioning of the instrumentation described below are shown in Fig. 2.

Owing to its pronounced seiching, Lake Alpnach has been the subject of numerous previous studies, emphasizing the structure and dynamics of the internal seiching (Münnich et al. 1992; Wüest et al. 2000), the seiche-induced BBL (Gloor et al. 1994; Lorke et al. 2002), as well as the control of sediment–water exchange by BBL turbulence (Lorke et al. 2003).

Thermistor string—A high-resolution thermistor string, assembled by using 17 individual TR1050 temperature loggers (RBR Ltd.), was deployed on the southwest slope of the lake at a depth of 31 m from 28 May–18 June 2003 (for positioning, *see Fig. 2*). The temperature measurements covered a depth range from 0.4 to 5.2 m above the sediment,

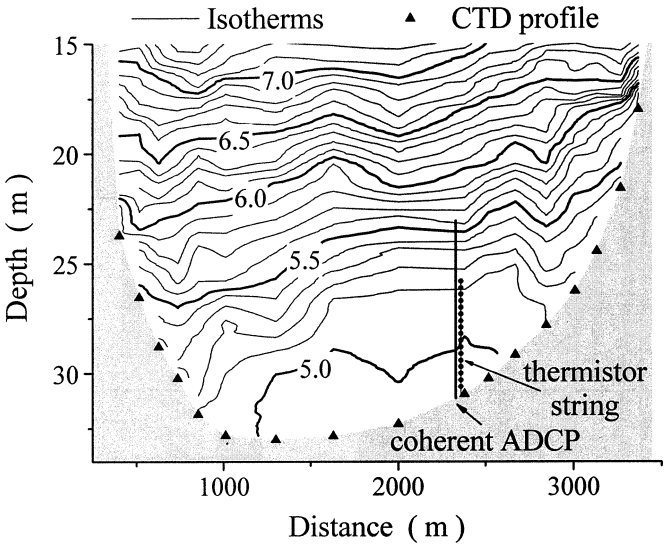

Fig. 2. Hypolimnetic temperature distribution along the main axis of Lake Alpnach, measured on 26 May 2003. Isotherms are plotted from 5.0–7.4°C in 0.1°C steps (numbers in the graph correspond to the respective temperature in degrees Celsius). The positions of the individual CTD casts and the position of the thermistor string and the ADCP are indicated.

with a spatial and temporal resolution of 0.3 m and 3 s (nominal response time <3 s), respectively. The data were averaged to series of 1-min time resolution for subsequent analysis.

The nominal accuracy and resolution of the TR1050 temperature loggers was $\pm 2 \times 10^{-3}$ °C and 5×10^{-5} °C, respectively, and the relative accuracy of the different thermistors was confirmed in the laboratory before and after deployment using a 7025 Benchtop Calibration Bath (Hart Scientific). The sensors were simultaneously calibrated by using an automated temperature stepping program. This allowed sensor-to-sensor differences to be reduced to $\sim 1 \times 10^{-3}$ °C.

The thickness of the well-mixed BBL was estimated from the thermistor data as the height above the bottom at which the vertical temperature gradient exceeded 0.03°C m^{-1}.

ADCP—A 614 kHz RDI Workhorse acoustic Doppler current profiler (ADCP, RD Instruments) was deployed at 31-m depth and ~50 m from the thermistor string (position in Fig. 2) for the entire period of measurements. The ADCP was operated in pulse-coherent mode (RDI mode 5), resolving a depth range from 0.59–8.49 m above the sediment with a cell size of 0.1 m. The profile interval was set to 10 s, whereby three individual pings were averaged internally for each profile and data were saved in beam coordinates. The horizontal current velocities were rotated in a horizontal plane to extract the velocity components along and perpendicular to the main axis of the lake. Positive along-lake velocities indicate upwelling and negative along-lake velocities indicate downwelling at the mooring site (Fig. 2).

Dissipation rates ε of TKE were estimated from the in-beam velocity spectra by using a modified inertial dissipation technique following the method of Lorke and Wüest

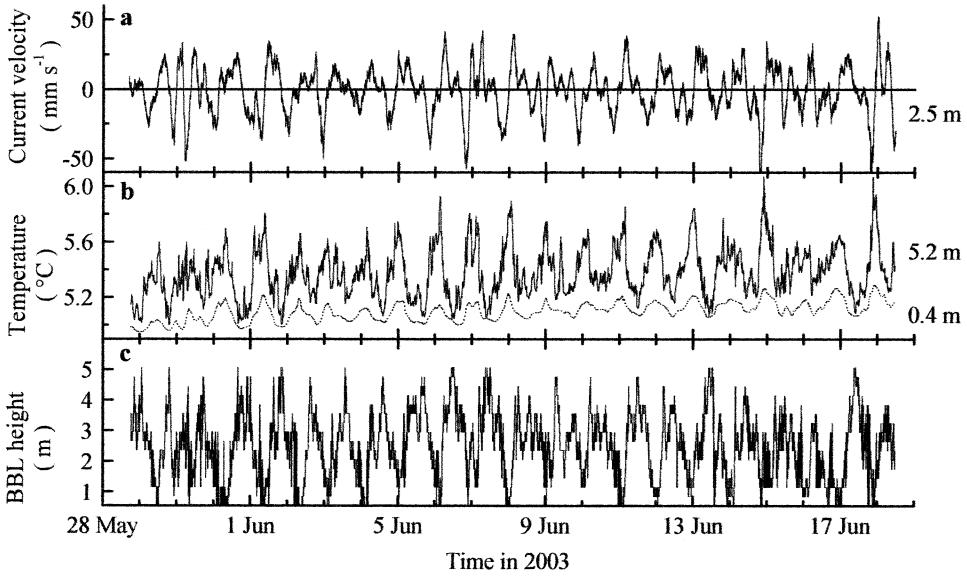

Fig. 3. (a) Time series of along-lake current velocities at 2.5 m above the sediment, (b) temperatures measured by the topmost (5.2 m above sediment) and lowest (0.4 m above sediment) thermistors, and (c) BBL height for the entire observation.

(2005). Wavenumber spectra were estimated from half-overlapping segments of 128 data points (21 min), and ε was obtained by fitting an inertial subrange to such spectra whenever the noise level was exceeded (Lorke and Wüest 2005).

CTD profiling—Vertical profiles of temperature, electrical conductivity, and light transmissivity were measured at 22 locations along a transect following the main axis of the lake on 26 May 2003 by using a SBE 9 CTD (conductivity, temperature, depth) probe (Sea-Bird Electronics). Positioning was achieved by global positioning system, and the total time to complete the transect was 1 h 20 min. The depths of selected isotherms along the transect were estimated by linear interpolation between individual profiles.

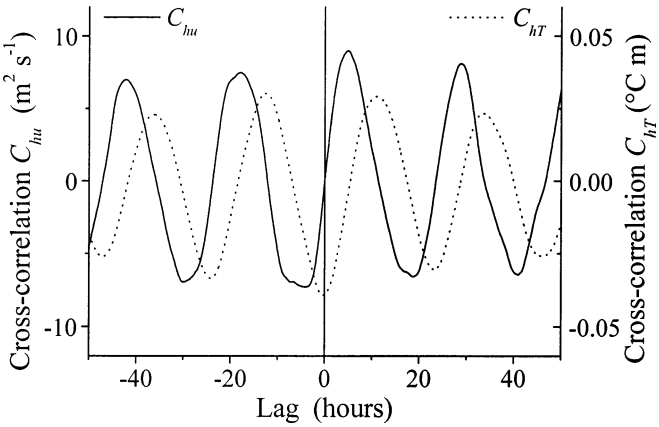

Fig. 4. Cross-correlation sequence C_{hu} of the BBL height h and the current velocity u_{long} at 1 m above the sediment (solid line) and cross-correlation sequence C_{hT} of BBL height and temperature at 0.4 m above the sediment (dotted line). The sequences were unbiased, and the lag was applied to h.

Observations and analyses

Spatial and temporal dynamics of the BBL—The hypolimnetic temperature distribution along the main axis of Lake Alpnach, shown in Fig. 2, was measured 2 d before the mooring deployment. The open-water column below 15-m depth was nearly linearly stratified down to ~30 m. Below 30-m depth, an up to 5-m-thick well-mixed BBL was observed. All isotherms, including the 5°C isotherm indicating the upper limit of the mixed BBL, were tilted owing to internal seiching or direct wind action. The time series of the along-lake current velocity, temperature, and BBL height measured with the moored instruments are depicted in Fig. 3 (for position of instruments, see Fig. 2). The time series reveal highly periodic and well-correlated fluctuations of temperature, stratification, and velocity.

The CTD transect in combination with the moored observations provides some insight into the spatial and temporal dynamics of the BBL. The major baroclinic motions were driven by internal seiching, leading to an almost parallel isotherm displacement in the hypolimnion with amplitudes of up to 5 m. As depicted in Fig. 2, the well-mixed BBL moved up and down the respective slope during the course of the oscillations.

BBL height and stratification observed at a certain time were not determined by local turbulence and mixing but by advection of the well-mixed BBL up and down the respective slope (Gloor et al. 2000). This feature becomes clear in the time series shown in Fig. 3 and particularly in the cross-correlations shown in Fig. 4. The cross-correlation sequences are periodic, with the seiching period of $\tau \approx 23.5$ h. The cross-correlation C_{hu} of the BBL height h and the near-bottom current velocity u_{long} shows a phase shift of ~6 h or $\tau/4$. Thus the maximum and minimum BBL heights coincided with the zero-crossings of the current velocity and hence

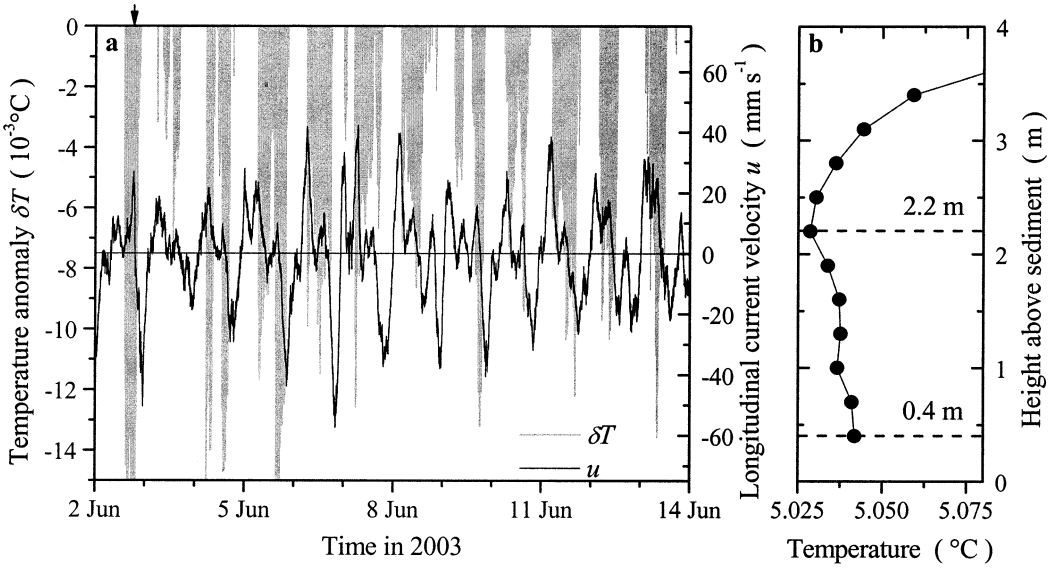

Fig. 5. (a) Time series of the along-lake current velocity u_{long} and the temperature anomaly δT, estimated as the difference between the temperatures measured at 2.2 and 0.4 m above the sediment. Note that only negative values of δT, representing unstable stratification, are shown. Positive current velocities were associated with up-slope currents at the mooring site (Fig. 2). For clarity of presentation, only a representative part of the entire observation is shown. (b) A temperature profile measured during unstable stratification (the sampling time is indicated by the arrow at the upper axis of Fig. 5a). The two dashed lines encompass the depth range used for calculating δT.

with the reversals of the seiche-induced motions. h lagged behind u_{long}, and maximum BBL heights were observed during the flow reversals after upwelling (positive current velocities) at the mooring site.

This conclusion is consistent with the cross-correlation sequence C_{hT} of the BBL height h and the near-bottom temperature (Fig. 4), which shows a phase shift of ~12 h, corresponding to $\pi/2$. Thus BBL height maxima were associated with temperature minima and hence with upwelling at the mooring site.

BBL stratification—Another feature of the BBL in Lake Alpnach was the periodic occurrence of inverse temperature stratification (Fig. 5). Because chemical stratification was shown to be negligible in the BBL of Lake Alpnach (Wüest and Gloor 1998), the observed temperature inversions represent gravitationally unstable conditions. Typically, unstable stratification was observed to extend over the entire BBL (up to 2 to 3 m above the sediment) with temperature anomalies δT, defined here as the temperature difference between 2.2 and 0.4 m above the sediment, as large as −0.015°C.

The temporal dynamics of the occurrence of inverse stratification was clearly linked to seiching (Fig. 5). Negative temperature anomalies, which indicate unstable stratification, were initiated when the along-lake current velocity u_{long} reached its positive maximum (maximum upslope current velocities at the mooring site) and had a maximum when the current velocity went through zero (changing from upslope to downslope current direction at the mooring site). In most cases, however, the unstable stratification persisted after the current direction reversed, and continued almost until the maximum downslope current velocity was reached.

Convective mixing and turbulence—Similar to convective mixing at the water surface, which is usually driven by a positive surface buoyancy flux, i.e., by heat loss at the water surface (Shay and Gregg 1986; Anis and Moum 1992; Jonas et al. 2003), gravitationally unstable stratification in the BBL can lead to sinking plumes of heavier water and rising plumes of lighter water and hence to the production of TKE and mixing. When buoyancy is generated by a density anomaly ρ', which is associated with a temperature anomaly δT, its ability to overcome viscous forces and thermal diffusion and hence give rise to active thermal convection is described by the Rayleigh number:

$$\text{Ra} = \frac{g\rho'}{\rho K_T \nu} h^3 \tag{1}$$

(Turner 1973), with g denoting the gravitational acceleration; K_T, the molecular diffusivity of heat; ν, the kinematic viscosity; and h, the height of the unstable layer. Calculating Ra for the typical observations described above (δT = 0.01°C, h = 2.5 m) results in Ra ≈ 10^8. This value exceeds the threshold for active convection (Ra ≈ 10^3, Turner 1973) found in laboratory experiments by several orders of magnitude.

In analogy to the surface layer, convective mixing is characterized by the buoyancy flux J_b^B, which is defined as

$$J_b^B = -\frac{g}{\rho}\langle \rho' w' \rangle \tag{2}$$

where $\langle \rho' w' \rangle$ denotes the Reynolds averaged cross-correlation of density (ρ') and vertical velocity (w') fluctuations (Turner 1973). For a convectively driven layer of height h and given that the density fluctuations ρ' are owing to tem-

perature variations $\alpha\rho T'$ (α is the coefficient of thermal expansion), the buoyancy flux (Eq. 2) is determined by

$$J_b^B = \frac{g}{\rho}\langle\rho' w'\rangle \approx \frac{g}{\rho} h \frac{d\rho}{dt} = g\alpha h \frac{DT}{Dt} \tag{3}$$

Relevant for the instability and convection in the BBL is the differential temperature change DT/Dt within layers along the cross-slope direction. The differential temperature change is zero at the sediment–water boundary and $DT/Dt = u(\partial T/\partial x)$ at the upper end of the BBL, with u being the velocity difference across the convective layer; $\partial T/\partial x$, the across-slope horizontal temperature gradient. In this temperature balance, the geothermal heat flux is neglected justifiably. The maximum buoyancy flux in the BBL is then given by

$$J_b^B = g\alpha h u \frac{\partial T}{\partial x} \tag{4}$$

Based on Fig. 2, the temperature gradient in the direction parallel to the slope was $\partial T/\partial x \sim 0.1$°C/250 m above the well-mixed BBL, i.e., above the 5.0°C isotherm. Using this estimate together with $h = 2.5$ m, $u = 3$ cm s^{-1} and $\alpha = 2.4 \times 10^{-5}$ °C^{-1} (at 5.5°C; according to the method of Chen and Millero [1986]) results in a buoyancy flux of $J_b^B \approx 7 \times 10^{-9}$ W kg^{-1} (Eq. 4). This estimate represents an upper bound of J_b^B, because the velocity difference $u = 3$ cm s^{-1} refers to the maximum current velocity throughout the seiching and to a linear interpolation from the bottom ($u = 0$) to the height of the convective layer h.

It should be noted that Eq. 4 is equivalent to the scaling argument introduced by Moum et al. (2004) by balancing the BBL buoyancy flux with the horizontal buoyancy advection:

$$J_b^B = \frac{g}{\rho}\int_0^H u \frac{\partial \rho}{\partial x}\, dz \tag{5}$$

Moum et al. (2004) measured the buoyancy flux in the BBL on the continental shelf, which exceeded our observed buoyancy flux J_b^B by one order of magnitude. They further used Eq. 5 to estimate the cross-slope current velocity u. The buoyancy flux on the continental shelf was much higher because of the thermal expansivity of seawater, which is also an order of magnitude larger than that for cold freshwater.

Following the method of Shay and Gregg (1986), the upper bound of J_b^B and the thickness h can be used to characterize the properties of turbulent convection. The convective timescale t_* is given by

$$t_* = \left(\frac{h^2}{J_b^B}\right)^{1/3} \tag{6}$$

Evaluating t_* for $h = 2.5$ m and $J_b^B \approx 7 \times 10^{-9}$ W kg^{-1} results in a lower bound for $t_* \approx 16$ min. Analogously, the velocity scale $w_* = (hJ_b^B)^{1/3}$ for convective turbulence is $w_* \approx 2.6$ mm s^{-1}.

If convective turbulence was an additional source of TKE, then dissipation rates ε should be enhanced during the cycle of unstable stratification. Dissipation rates were calculated from the ADCP data following the method of Lorke and Wüest (2005). However, a 614-kHz ADCP is unable to resolve the entire dynamic range of turbulent energy dissipation in low-energetic environments. Values for ε could only be reliably estimated for relatively strong dissipation, which covered ~50% of the entire period of measurements. The statistics of the dissipation rate estimates as a function of the observed temperature anomaly are shown in Fig. 6. Whereas the mean dissipation rate did not show a significant dependence on δT ($\langle\varepsilon_{mean}\rangle \approx 8 \times 10^{-10}$ W kg^{-1} for $\delta T < 0$ and $\langle\varepsilon_{mean}\rangle \approx 5 \times 10^{-10}$ W kg^{-1} for $\delta T > 0$), its maximum value decreased with increasing δT ($\langle\varepsilon_{max}\rangle \approx 5 \times 10^{-9}$ W kg^{-1} for $\delta T < 0$ and $\langle\varepsilon_{max}\rangle \approx 2 \times 10^{-9}$ W kg^{-1} for $\delta T > 0$), given an accuracy of the dissipation rate estimates within a factor of two (Lorke and Wüest 2005). However, the number of valid dissipation rate estimates, and hence the instances of more energetic turbulence showed a strong increase during unstable stratification ($\delta T < 0$) with a peak at $\delta T \approx -0.005$°C.

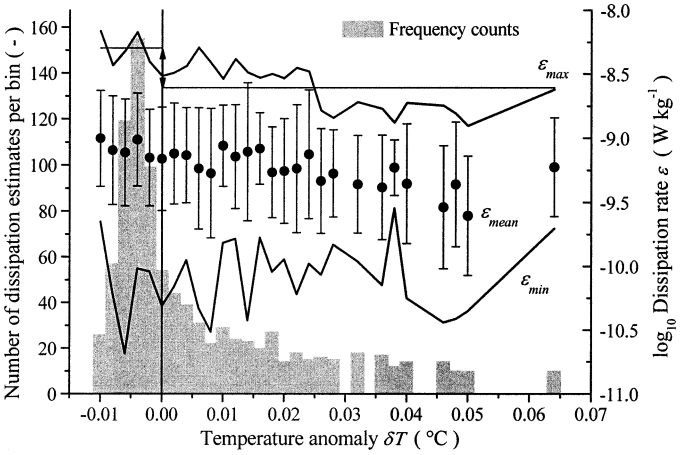

Fig. 6. Bin mapping of the dissipation rate estimates ε measured 0.8 m above the sediment as a function of the observed temperature anomaly δT (negative values represent unstable stratification). The data points show the mean dissipation rates (ε_{mean}) with their logarithmic standard deviation (intermittency), and the lines show the observed maximum (ε_{max}) and minimum (ε_{min}) dissipation rates. The grey bars are the associated numbers of occurrence per bin. The overall mean of ε_{max} increased from $\langle\varepsilon_{max}\rangle = 2 \times 10^{-9}$ W kg^{-1} for $\delta T > 0$ to $\langle\varepsilon_{max}\rangle = 5 \times 10^{-9}$ W kg^{-1} for $\delta T < 0$, as indicated by the two horizontal lines. This difference is nearly equal to 1.5 J_b^B.

Discussion

Shear-induced convection on slopes—The periodic occurrence of unstable BBL stratification can be explained by differential transport of water masses close to the sediment surface across the slope. In a simplified view, the velocity profile in the BBL is assumed to follow law-of-the-wall scaling; i.e., the velocity increases logarithmically with distance from the sediment (Wüest and Lorke 2003*b*). It is further assumed that the isotherms (isopycnals) intersect the sediment surface at a right angle. It thus follows directly from the boundary condition that turbulent fluxes should vanish at the water-sediment interface (Thorpe 1987).

The dynamics of such a BBL, which is periodically forced

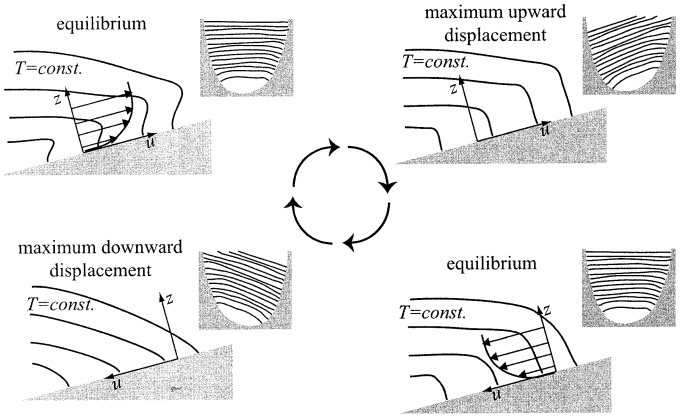

Fig. 7. Schematic illustration of the generation of unstable stratification on a slope by a complete cycle of internal seiching. The small panels show the respective phase of the internal seiching expressed as isotherm displacements along the main cross-section of the lake (in accordance to the measurements depicted in Fig. 2, note that only the hypolimnion is shown). The four main panels show the detailed characteristics of isotherms (T = *const.*) and current velocity (u) in the BBL on a right-hand slope (again in accordance to Fig. 2).

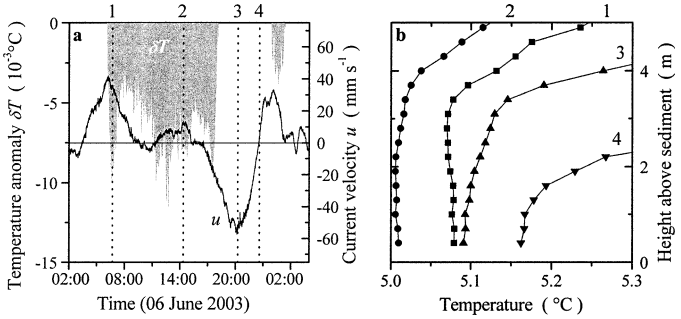

Fig. 8. (a) Section of the time series of current velocity u_{long} and temperature anomaly δT taken from Fig. 5 exemplifying one complete cycle of internal seiching. (b) Temperature measured at the respective times, indicated by the numbers (1–4 in Fig. 8a).

by seiching, is illustrated in Fig. 7. Unstable stratification is generated during the phase of cold-water upwelling on the slope. Because the water at some distance from the bottom is transported faster than is the water near to the sediment surface, colder water is moved above warmer water in the BBL, leading to unstable stratification and convective mixing. According to the assumptions made, the unstable stratification should relax and the stratification in the BBL should become stable after the maximum seiche-induced displacement is reached, i.e., after the along-lake current velocity passes through zero. During the phase of downwelling, the same differential transport mechanism as described above moves warmer water downslope from shallower regions on top of colder water flowing more slowly near the sediments. This leads to stable and rather strong stratification in the BBL on the slope.

The features depicted in Fig. 7 and described above are supported by temperature profiles measured during a seiching cycle (Fig. 8). Unstable stratification is initiated during the highest upwelling velocities, and the BBL is reduced to a thin, stably stratified layer when downwelling is strongest. However, the observations have revealed that the unstable stratification in the BBL did not vanish directly after the cease of upslope flow but continued to persist into the phase of downslope motion (Figs. 5, 8). This behavior can be explained by the special form of the velocity profiles in a periodically forced BBL, which does not follow classical law-of-the-wall characteristics as assumed in the simplified model presented above. Lorke et al. (2002) showed that periodic forcing leads to a BBL that follows the characteristics of Stokes' oscillatory boundary layer (Stokes 1845; Schlichting 1962), and that the law-of-the-wall scaling cannot be applied to describe the form of the near-bed current velocity profile.

The temporal evolution of the current velocity profiles observed during the transition from upwelling to downwelling is shown in Fig. 9 for the sampling period depicted in Fig. 8. These current profiles illustrate deviation from the log-layer structure through their characteristic velocity maximum at some distance from the sediment. Velocity profiles observed during other downwelling phases even showed a maximum current speed near the sediment. This special form of the velocity profiles leads to the transport of warmer water from shallower regions downslope. Water at the depth of the current velocity maximum is transported faster than is the water above and hence, eventually, leads to transport of warmer water below colder water. Thus, the unstable stratification and convective mixing is still maintained at the beginning of the downwelling period. The latter mechanism is comparable to the one suggested by Moum et al. (2004), who observed convectively driven mixing in the BBL on a continental shelf and attributed this process to Ekman-induced downwelling.

Further support of the above proposed mechanism for the formation of unstable stratification is provided by direct es-

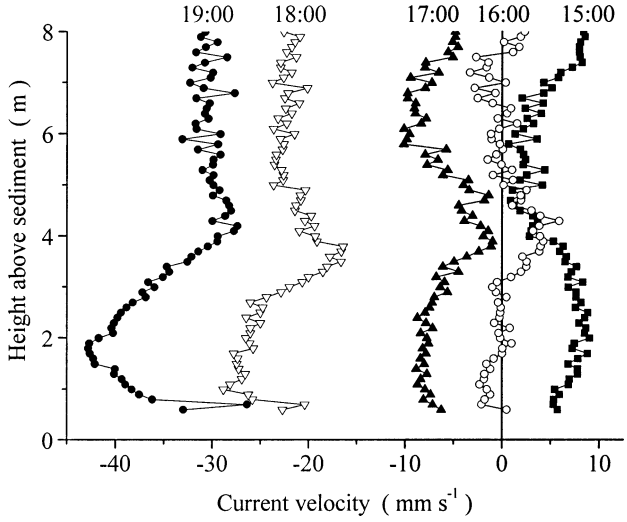

Fig. 9. Temporal evolution of the current velocity profiles during the transition from up- to downwelling. The profiles were measured on 6 June 2003 between 1500 and 1900 h and characterize the transition from 2 to 3 in Fig. 8.

timates of the differential transport of water masses in the BBL. Temporal integration of the measured along-lake currents at different heights above the sediment provides the travel distances for the respective water masses. The difference between the distance traveled by water at 0.59 m and the distance traveled at 2.59 m above the bottom was up to 250 m during half of a seiching period, i.e., during an entire phase of up- or downwelling at the mooring site. Comparison with Fig. 2 shows that a cross-slope distance of 250 m is associated with a horizontal temperature gradient of ~0.1°C within the stratified part of the hypolimnion and thus supports the shear-induced convection scenario discussed above.

Buoyancy flux and turbulence dissipation—The high Rayleigh number and the estimated time scale for turbulent convection of only ~16 min, which is short compared with the persistence of the observed static instabilities, indicate that shear-induced convection led to buoyancy-driven turbulence during our observations.

In analogy to surface layer convection, the dissipation rate of convective turbulence scales with the buoyancy flux (Shay and Gregg 1986). If no mechanical energy is radiated away, the layer-averaged dissipation is determined purely by energetic arguments and given by $\langle \varepsilon \rangle = 0.5\ J_b^B$. Field measurements in lakes and oceans (*see* Imberger 1985; Shay and Gregg 1986; Anis and Moum 1992), revealing dissipation rates between 0.3 and 0.8 J_b^B, have confirmed this relation well within the usual systematic uncertainties of the methods. Our observations are also concurrent: The maximum buoyancy flux (Eq. 4), observed during the cycle of convective mixing ($\delta T < 0$, Fig. 6), was $J_b^B \sim 7 \times 10^{-9}$ W kg^{-1} (see above), and the maximum dissipation rate $\langle \varepsilon_{max} \rangle \sim 5 \times 10^{-9}$ W kg^{-1} $\sim 0.7\ J_b^B$ was consistent with $0.5\ J_b^B$. Within the experimental uncertainty, turbulence measurements and the maximum buoyancy flux, estimated from the background stratification and flow, agreed well with common convective scaling.

Two important conclusions can be drawn from this agreement. First, a clear distinction between shear-induced and buoyancy-driven turbulence in the BBL on the slope was not possible. Because the maximum dissipation rate increased by only a factor of two during convective mixing ($\delta T < 0$) (Fig. 6), it can be concluded that bottom shear production and buoyancy-driven (convective) production contributed by similar amounts to the TKE, and hence their presence or absence could not be reliably detected using turbulence measurements.

Second, the equal contribution of shear-induced and buoyancy-driven turbulence emphasizes the importance of shear-induced convection on sloping boundaries. Most attempts to budget the production of TKE and associated mixing processes in lakes (Imberger 1998; Wüest et al. 2000) and ocean basins (Garrett 2003; Wunsch and Ferrari 2004) have revealed the importance of BBL turbulence for basin-scale mixing processes, although the only processes considered were shear production and the breaking of internal waves. Further observational and numerical research into the process of shear-induced convection should investigate its parameterization in terms of stratification and bottom slope and cross-slope current velocity and hence result in an assessment of its importance for boundary mixing in different environments.

References

ANIS, A., AND J. N. MOUM. 1992. The superadiabatic surface layer of the ocean during convection. J. Phys. Oceanogr. **22:** 1221–1227.

CALDWELL, D. R. 1978. Variability of the bottom mixed layer on the Oregon shelf. Deep-Sea Res. **25:** 1235–1243.

CHEN, C.-T. A., AND F. J. MILLERO. 1986. Precise thermodynamic properties for natural waters covering only the limnological range. Limnol. Oceanogr. **31:** 657–662.

FRICKER, P. D., AND H. M. NEPF. 2000. Bathymetry, stratification, and internal seiche structure. J. Geophys. Res. **105:** 14237–14251.

GARRETT, C. 1991. Marginal mixing theories. Atmosphere Ocean **29:** 313–339.

———. 2003. Internal tides and ocean mixing. Science **301:** 1858–1859.

GLOOR, M., A. WÜEST, AND D. IMBODEN. 2000. Dynamics of mixed bottom boundary layers and its implications for diapycnal transport in a stratified, natural water basin. J. Geophys. Res. **105:** 8629–8646.

———, ———, AND M. MÜNNICH. 1994. Benthic boundary mixing and resuspension induced by internal seiches. Hydrobiologia **284:** 59–68.

GOUDSMIT, G.-H., F. PEETERS, M. GLOOR, AND A. WÜEST. 1997. Boundary versus diapycnal mixing in stratified natural waters. J. Geophys. Res. **102:** 27903–27914.

HONDZO, M., AND Z. HAIDER. 2004. Boundary mixing in a small stratified lake. Water Resour. Res. **40.** [doi:10.1029/2002WR001851]

IMBERGER, J. 1985. The diurnal mixed layer. Limnol. Oceanogr. **30:** 737–770.

———. 1998. Flux paths in a stratified lake: A review, p. 1–18. *In* J. Imberger [ed.], Physical processes in lakes and oceans. Coastal and Estuarine Studies. American Geophysical Union.

———, AND G. N. IVEY. 1993. Boundary mixing in stratified reservoirs. J. Fluid Mech. **248:** 477–491.

JONAS, T., A. STIPS, W. EUGSTER, AND A. WÜEST. 2003. Observations of a quasi shear-free lacustrine convective boundary layer: Stratification and its implications on turbulence. J. Geophys. Res. **108(C10).** [doi:10.1029/2002JC001440]

LEDWELL, J. R., AND A. BRATKOVICH. 1995. A tracer study of mixing in the Santa Cruz Basin. J. Geophys. Res. **100:** 20681–20704.

———, AND B. M. HICKEY. 1995. Evidence for enhanced boundary mixing in the Santa Monica Basin. J. Geophys. Res. **100:** 20665–20679.

———, E. T. MONTGOMERY, K. L. POLZIN, L. C. ST-LAURENT, R. W. SCHMITT, AND J. M. TOOLE. 2000. Evidence for enhanced mixing over rough topography in the abyssal ocean. Nature **403:** 179–182.

LEMCKERT, C., J. P. ANTENUCCI, A. SAGGIO, AND J. IMBERGER. 2004. Physical properties of turbulent benthic boundary layers generated by internal waves. J. Hydraul. Eng. **130:** 58–69.

LENTZ, S. J., AND J. H. TROWBRIDGE. 1991. The bottom boundary layer over the northern California shelf. J. Phys. Oceanogr. **21:** 1186–1201.

LORKE, A., B. MÜLLER, M. MAERKI, AND A. WÜEST. 2003. Breathing sediments: The control of diffusive transport across the sediment–water interface by periodic boundary-layer turbulence. Limnol. Oceanogr. **48:** 2077–2085.

———, L. UMLAUF, T. JONAS, AND A. WÜEST. 2002. Dynamics of turbulence in low-speed oscillating bottom-boundary layers of stratified basins. Environ. Fluid Mech. **2:** 291–313.

———, AND A. WÜEST. In press. Application of coherent ADCP for turbulence measurements in the bottom boundary layer. J. Atmos. Oceanic Technol.

MACINTYRE, S., K. M. FLYNN, R. JELLISON, AND J. R. ROMERO. 1999. Boundary mixing and nutrient fluxes in Mono Lake, California. Limnol. Oceanogr. **44:** 512–529.

MOUM, J. N., A. PERLIN, J. M. KLYMAK, M. D. LEVINE, T. BOYD, AND P. M. KOSRO. 2004. Convectively-driven mixing in the bottom boundary layer. J. Phys. Oceanogr. **34:** 2189–2202.

MÜLLER, P., AND C. GARRETT. 2004. Near-boundary processes and their parameterization. Oceanography **17:** 107–116.

MÜNNICH, M., A. WÜEST, AND D. M. IMBODEN. 1992. Observation of the second vertical mode of the internal seiche in an alpine lake. Limnol. Oceanogr. **37:** 1705–1719.

PHILLIPS, O. M. 1970. On flows induced by diffusion in a stably stratified fluid. Deep-Sea Res. **17:** 435–443.

RIPPETH, T. P., N. R. FISHER, AND J. H. SIMPSON. 2001. The cycle of turbulent dissipation in the presence of tidal straining. J. Phys. Oceanogr. **31:** 2458–2471.

RUDNICK, D. L., AND OTHERS. 2003. From tides to mixing along the Hawaiian Ridge. Science **301:** 355–357.

SCHLICHTING, H. 1962. Boundary layer theory, 6th ed. McGraw-Hill.

SHAY, T. J., AND M. C. GREGG. 1986. Convectively driven mixing in the upper ocean. J. Phys. Oceanogr. **16:** 1777–1799.

SIMPSON, J. H. 1997. Physical processes in the ROFI regime. J. Mar. Syst. **12:** 3–15.

———, J. BROWN, J. MATTHEWS, AND G. ALLEN. 1990. Tidal straining, density currents, and stirring in the control of estuarine stratification. Estuaries **13:** 125–132.

SLINN, D. N., AND M. D. LEVINE. 2003. Modeling internal tides and mixing over ocean ridges, p. 59–68. *In* P. Müller and D. Henderson [eds.], Thirteenth 'Aha Huliko'a Hawaiian Winter Workshop on Near Boundary Processes and their Parameterization. SOEST Special Publication.

STACEY, M. T., S. MONISMITH, AND J. R. BURAU. 1999. Observation of turbulence in a partially stratified estuary. J. Phys. Oceanogr. **29:** 1950–1970.

STOKES, G. G. 1845. On the theories of the internal friction of fluids in motion. Trans. Cambridge Philos. Soc. **8:** 287–319.

THORPE, S. A. 1987. Current and temperature variability on the continental slope. Philos. Trans. R.Soc. Lond. B Biol. Sci. **A323:** 471–517.

———. 1997. On the interaction of internal waves reflecting from slopes. J. Phys. Oceanogr. **27:** 2072–2078.

TROWBRIDGE, J. H., AND S. J. LENTZ. 1991. Asymmetric behavior of an oceanic boundary layer above sloping bottom. J. Phys. Oceanogr. **21:** 1171–1185.

TURNER, J. S. 1973. Buoyancy effects in fluids. Cambridge Univ. Press.

WEATHERLY, G. L., AND P. J. MARTIN. 1978. On the structure and dynamics of the oceanic bottom boundary layer. J. Phys. Oceanogr. **8:** 557–570.

WÜEST, A., AND M. GLOOR. 1998. Bottom boundary mixing: The role of near-sediment density stratification, p. 485–502. *In* J. Imberger [ed.], Physical processes in lakes and oceans. Coastal and Estuarine Studies. American Geophysical Union.

———, AND A. LORKE. 2003*a*. The effect of the bottom boundary on diapycnal mixing in enclosed basins, p. 9–15. *In* P. Müller and D. Henderson [eds.], Thirteenth 'Aha Huliko'a Hawaiian Winter Workshop on Near Boundary Processes and their Parameterization. SOEST Special Publication.

———, AND ———. 2003*b.* Small-scale hydrodynamics in lakes. Ann. Rev. Fluid Mech. **35:** 373–412.

———, G. PIEPKE, AND D. C. VAN SENDEN. 2000. Turbulent kinetic energy balance as a tool for estimating vertical diffusivity in wind-forced stratified waters. Limnol. Oceanogr. **45:** 1388–1400.

WUNSCH, C. 1970. On oceanic boundary mixing. Deep-Sea Res. **17:** 293–301.

———, AND R. FERRARI. 2004. Vertical mixing, energy, and the general circulation of the oceans. Ann. Rev. Fluid Mech. **36:** 281–314.

Received: 30 September 2004
Accepted: 14 Mar 2005
Amended: 2 May 2005